UC Irvine
UC Irvine Previously Published Works

Title

AMPK Activation by Metformin Suppresses Abnormal Extracellular Matrix Remodeling in Adipose Tissue and Ameliorates Insulin Resistance in Obesity.

Permalink

https://escholarship.org/uc/item/3mm5t8k2

Journal

Diabetes, 65(8)

Authors

Luo, Ting
Nocon, Allison
Fry, Jessica
et al.

Publication Date

2016-08-01

DOI

10.2337/db15-1122

Peer reviewed

Ting Luo,[1,2] Allison Nocon,[1] Jessica Fry,[1] Alex Sherban,[1] Xianliang Rui,[1]
Bingbing Jiang,[1] X. Julia Xu,[1] Jingyan Han,[1] Yun Yan,[3] Qin Yang,[4] Qifu Li,[2]
and Mengwei Zang[1,5,6,7]

AMPK Activation by Metformin Suppresses Abnormal Extracellular Matrix Remodeling in Adipose Tissue and Ameliorates Insulin Resistance in Obesity

Fibrosis is emerging as a hallmark of metabolically dysregulated white adipose tissue (WAT) in obesity. Although adipose tissue fibrosis impairs adipocyte plasticity, little is known about how aberrant extracellular matrix (ECM) remodeling of WAT is initiated during the development of obesity. Here we show that treatment with the antidiabetic drug metformin inhibits excessive ECM deposition in WAT of ob/ob mice and mice with diet-induced obesity, as evidenced by decreased collagen deposition surrounding adipocytes and expression of fibrotic genes including the collagen cross-linking regulator *LOX*. Inhibition of interstitial fibrosis by metformin is likely attributable to the activation of AMPK and the suppression of transforming growth factor-β1 (TGF-β1)/Smad3 signaling, leading to enhanced systemic insulin sensitivity. The ability of metformin to repress TGF-β1-induced fibrogenesis is abolished by the dominant negative AMPK in primary cells from the stromal vascular fraction. TGF-β1-induced insulin resistance is suppressed by AMPK agonists and the constitutively active AMPK in 3T3L1 adipocytes. In omental fat depots of obese humans, interstitial fibrosis is also associated with AMPK inactivation, TGF-β1/Smad3 induction, aberrant ECM production, myofibroblast activation, and adipocyte apoptosis. Collectively, integrated AMPK activation and TGF-β1/Smad3 inhibition may provide a potential therapeutic approach to maintain ECM flexibility and combat chronically uncontrolled adipose tissue expansion in obesity.

In obesity, visceral adipose tissue dysfunction contributes to the development of insulin resistance and type 2 diabetes mellitus. Physiologically, extracellular matrix (ECM) components such as collagens and fibronectin provide mechanical support for tissue. As obesity-induced adipose tissue expansion progresses, chronic, continuous production and deposition of ECM lead to the destruction of normal adipose tissue architecture, which is referred to as adipose tissue ECM remodeling (1). Genetic deletion of collagen VI (Col6a3), which is highly expressed in adipose tissue, improves adipose fibrosis and systemic metabolic dysfunction in mice fed a high-fat diet, highlighting the critical role of adipose tissue ECM in regulating metabolic homeostasis (2). Adipose tissue fibrosis is increasingly appreciated as a major contributor of metabolic dysregulation in obese humans and those with type 2 diabetes (3). However, how persistent aberrant ECM remodeling is initiated by obesity remains poorly understood. The major goal of this study is to identify the signaling molecules that modulate fat tissue ECM remodeling in obesity.
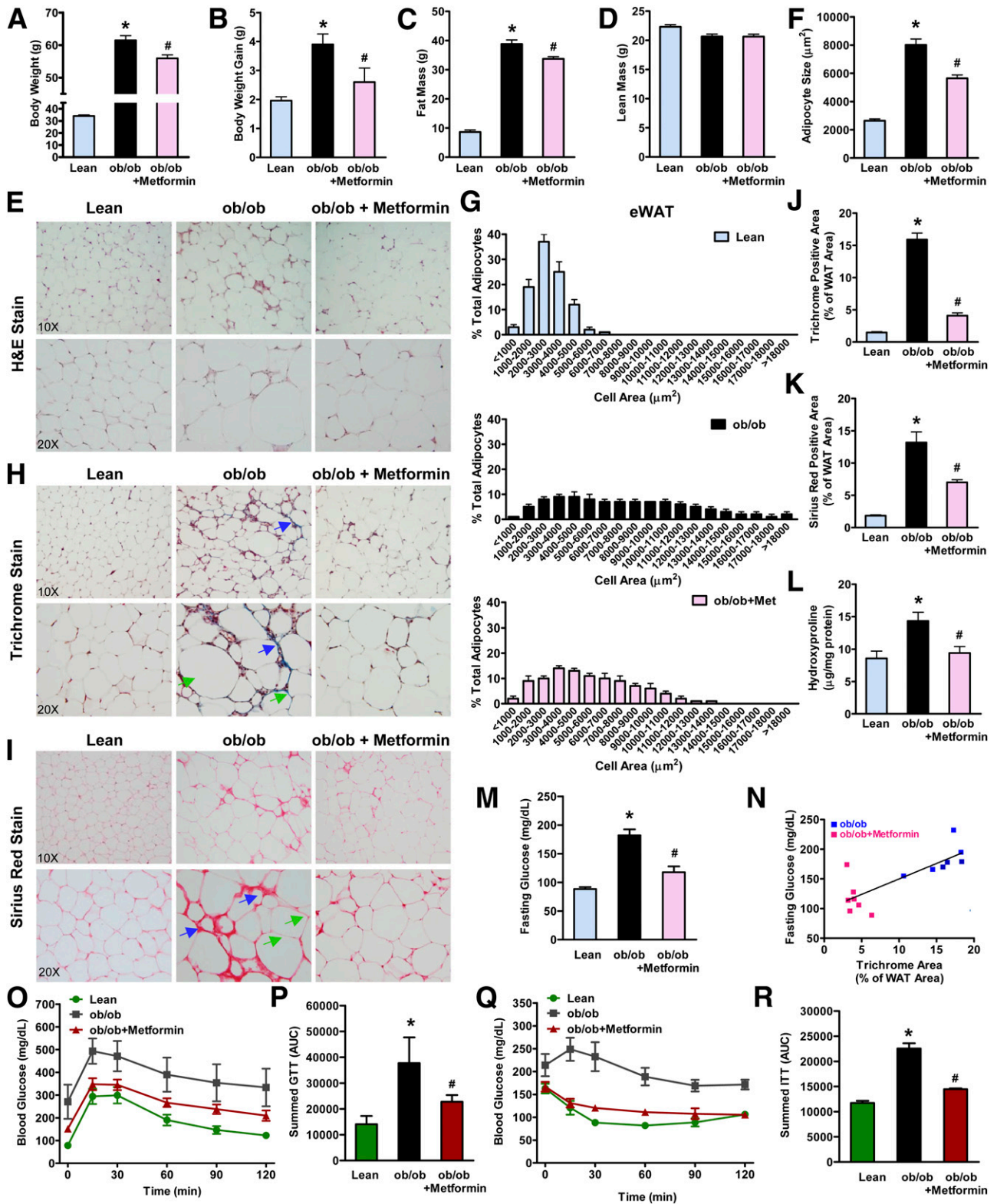
OBESITY STUDIES

Figure 1—Metformin treatment reduces body weight gain, decreases adiposity, and relieves excessive collagen deposition in WAT of genetically obese ob/ob mice. A and B: Administration of metformin (250 mg/kg/day) for 4 weeks causes a moderate but significant body weight loss in ob/ob mice. Mice were divided into three groups: lean littermates (n = 15), ob/ob mice (n = 11), and ob/ob mice treated with metformin (ob/ob + Metformin; n = 10). C and D: Body composition in the three groups of mice. E: Representative H-E staining of eWAT of the mice. F: Average adipocyte areas of eWAT in H-E-stained sections, calculated using ImageJ software (National Institutes of Health, Bethesda, MD). G: The bar graphs represent adipocyte size distribution in eWAT of three groups of mice (n = 5–6 mice per group; >500 cells counted per group). H and I: Representative images of Masson trichrome staining (collagen is shown as blue, nuclei as black, and cytoplasm as red) and Sirius Red staining (collagen is shown as red) show the fibrotic structural characteristics in epididymal fat depots of

Metformin is the first-line drug that treats obesity-related type 2 diabetes (4,5). Our initial studies and others indicate that the lipid-lowering effect of metformin is largely attributable to the activation of AMPK, the energy sensor, in hepatocytes (6–9). Furthermore, metformin can repress de novo lipogenesis in hepatocytes by activating AMPK (10). Although the adipose tissue acts as a target of AMPK and its activator metformin (11–14), whether AMPK regulates adipose tissue ECM homeostasis remains undefined.

We report here that the interplay of AMPK and transforming growth factor (TGF)-β1 signaling is implicated in pericellular fibrosis in the omental fat of obese humans. Activation of AMPK by metformin suppresses TGF-β1/Smad3 signaling, resolves the interstitial accumulation of ECM in white adipose tissue (WAT), and improves local and systemic insulin resistance in animals with genetic and diet-induced obesity. Pharmacological and molecular activation of AMPK inhibits collagen induction, lysyl oxidase (LOX)–related collagen cross-linking, myofibroblast-like cell differentiation, and adipocyte apoptosis and insulin resistance upon TGF-β1 treatment in vitro. Targeting adipose tissue ECM may benefit adipose and whole-body insulin resistance in obesity.

RESEARCH DESIGN AND METHODS

Animal Studies
Male 8- to 10-week-old ob/ob C57BL/6 mice, as well as their lean littermates and wild-type mice, were purchased from The Jackson Laboratory (Bar Harbor, ME). All animal experiments were approved by the Institutional Animal Care and Use Committee at Boston University School of Medicine.

Primary Cell Culture from the Stromal Vascular Fraction of Adipose Tissue
Stromal vascular fraction (SVF) cells in epididymal fat depots from male C57BL/6 mice were isolated and cultured as described previously (15,16).

Human Studies
Omental adipose tissue samples were collected from obese patients (BMI 28.7 ± 1.4 kg/m^2) and age-matched normal-weight individuals (BMI 19.8 ± 1.5 kg/m^2). The ethics committee of the First Affiliated Hospital of Chongqing Medical University in China approved the study (IRB#15–39). Subjects gave written informed consent after individual explanation.

Statistical Analysis
Data are presented as mean ± SEM. Using GraphPad Prism 5.0 software, results were analyzed by one-way ANOVA (between multiple groups), when appropriate, and by a two-tailed Student t test (between two groups), as described previously (6,8,10,17–20). $P < 0.05$ was considered statistically significant.

RESULTS

Metformin Reduces Adiposity, Alleviates Excessive Collagen Deposition in WAT, and Ameliorates Whole-Body Insulin Resistance in Genetically Obese ob/ob Mice
As shown in Fig. 1, body weight gain was moderately but significantly reduced in metformin-treated ob/ob mice, as was seen in early studies (21). While lean mass was unaffected by metformin, the weight loss was mainly attributed to a 14% decrease in the fat mass of ob/ob mice, consistent with a moderate weight loss and fat mass reduction in patients with type 2 diabetes after metformin treatment (14,22,23). Histologically, hematoxylin-eosin (H-E) staining showed that metformin lessened features of hypertrophic adipocytes in epididymal WAT (eWAT) of ob/ob mice, with a switch toward smaller adipocytes. Masson trichrome staining showed an approximately sevenfold increase in collagen deposition and distinct distribution patterns of interstitial collagen in eWAT of ob/ob mice, in which fibrous regions appeared denser and thicker and gave rise to a larger lobe or a lobule-like structure. Sirius Red staining further confirmed that collagen fibers were mainly organized in fibrotic bundles surrounding adipocytes in ob/ob mice. Strikingly, abnormal collagen deposition was reduced approximately 50% in metformin-treated ob/ob mice. Quantification of hydroxyproline concentrations is considered an accurate indicator of tissue collagen content (24–26). An increase in hydroxyproline content in the eWAT of ob/ob mice was also reduced by metformin, reaching a concentration comparable with that of lean mice. Thus metformin protects against adiposity and pronounced ECM remodeling caused by obesity.

---

obese mice. Collagen fibers were organized in bundles of various thicknesses. Thinner collagen fibrils were also seen in the interstitial space between adipocytes, demonstrating pericellular fibrosis in fat depots. Thicker collagen fibers surrounding hypertrophic adipocytes were located in macrophage-abundant areas (blue arrows) in the stromal space of ob/ob mice. Notably, interstitial deposition of collagen fibrils around adipocytes was also evident in non-macrophage–rich regions (green arrows) of ob/ob mice. Original magnification ×10 and ×20. *J* and *K*: The bar graphs represent relatively positive-stained areas of the total tissue areas, calculated by ImageJ software (National Institutes of Health). *L*: Hydroxyproline content of epididymal fat, an indicator of total collagen content. *M*: Metformin lowers fasting blood glucose concentrations in ob/ob mice. *N*: Areas of collagen-positive staining in WAT are correlated with fasting glucose concentrations in ob/ob mice treated or untreated with metformin (R^2 = 0.6323; P = 0.0007). *O*: Glucose tolerance tests (GTTs) (glucose 2 g/kg intraperitoneally) in mice following a 16-h fast. *P*: Areas under the curve (AUC) for GTTs were estimated by summing the numerical integration values of successive linear segments of the glucose disposal curve above baseline glucose (n = 7–8). *Q*: Insulin tolerance tests (ITTs) (insulin 0.75 units/kg intraperitoneally) in mice following a 6-h fast. *R*: Summed ITT results from *Q* (n = 5–6). The data are presented as mean ± SEM (n = 7). *P < 0.05 vs. control mice; #P < 0.05 vs. ob/ob mice.
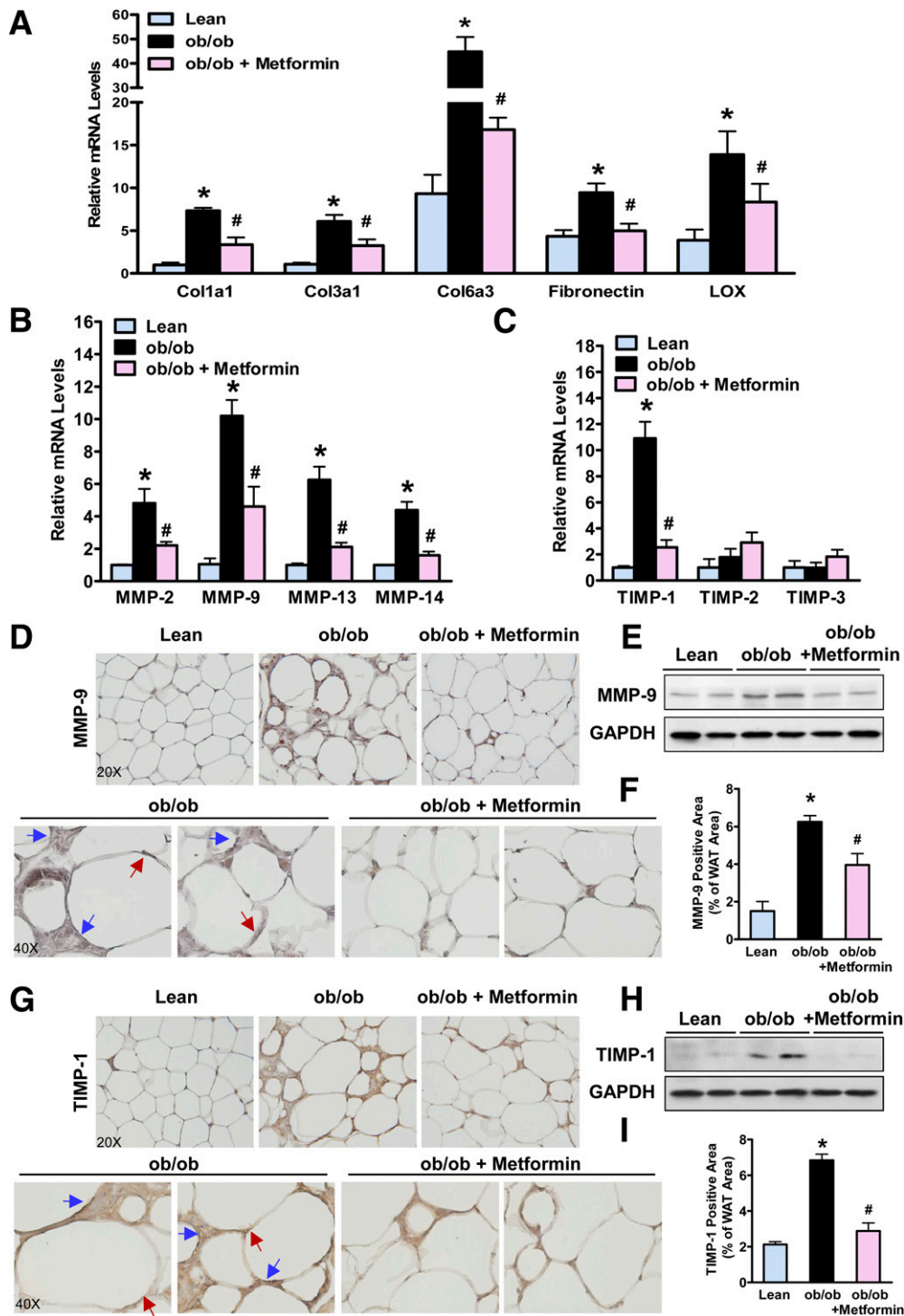
Figure 2—Metformin administration ameliorates abnormal synthesis and degradation of ECM components in WAT of ob/ob mice. *A*: The transcription of fibrogenic genes encoding Col1a1, Col3a1, Col6a3, fibronectin, and the collagen cross-linking enzyme LOX in epididymal fat are induced in ob/ob mice and suppressed by metformin. *B* and *C*: The mRNA levels of MMP-2, MMP-9, MMP-13, and MMP-14, as well as TIMP-1, TIMP-2, and TIMP-3, in eWAT of three groups of mice are measured by quantitative RT-PCR. *D–I*: Identification of possible ECM regulators involved in fat fibrosis. Representative immunohistochemical staining and immunoblots for MMP-9 (*D–F*) and TIMP-1 (*G–I*) are shown. Positive immunostaining appeared a brown color, similar to a collagen distribution pattern in fat depots. Notably, positive staining for MMP-9 and TIMP-1 was visualized mainly in some of adipocytes (red arrows) and other cells (blue arrows) in the stromal space of ob/ob mice. The induction of MMP-9 and TIMP-1 was decreased in metformin-treated mice (ob/ob + Metformin). The minimal staining was noted in lean littermates. There was no detectable staining with a nonspecific IgG isotype control in the adjacent adipose tissue sections (data not shown), indicating the specificity of MMP-9 and TIMP-1 staining. Original magnification ×20 and ×40. The bar graphs represent relatively positive-stained areas of the total tissue areas. The data are presented as mean ± SEM (*n* = 7). *$P < 0.05$ vs. lean mice; #$P < 0.05$ vs. ob/ob mice.
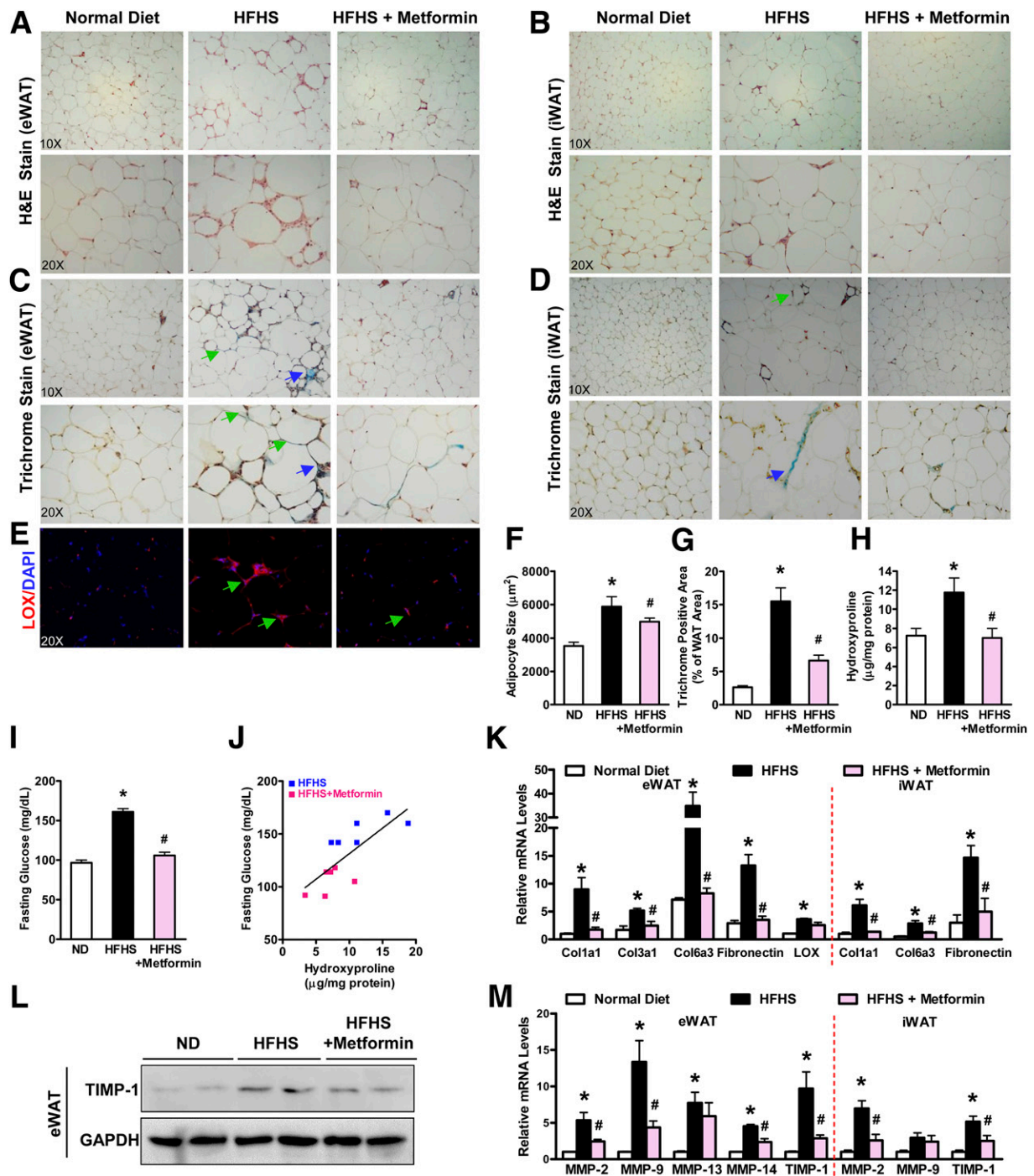
Figure 3—Metformin treatment inhibits abnormal interstitial deposition of collagens in WAT of a mouse model of HFHS diet–induced obesity. Mice were fed a normal chow diet (ND; $n = 7$), an HFHS diet ($n = 7$), or an HFHS diet supplemented with metformin (HFHS + Metformin; $n = 7$). Metformin-treated mice were initially fed an HFHS diet for 8 weeks, followed by HFHS feeding plus metformin treatment (250 mg/kg/day) for an additional 4 weeks. A and B: Representative H-E staining of eWAT and iWAT. C and D: Representative Masson trichrome staining of eWAT (C) and iWAT (D). Notably, interstitial deposition of collagen fibrils around adipocytes was evident in both macrophage-rich (blue arrows) and non-macrophage–rich regions (green arrows). E: Representative immunofluorescent staining for LOX (red) and nuclear staining with DAPI (blue). Notably, immunostaining for LOX displayed a pattern similar to the collagen distribution of obese mice (green arrows). Original magnification ×10 or ×20. F: Administration of metformin reduces adiposity in C57BL/6 mice fed the HFHS diet. The average adipocyte areas of eWAT were measured. G: The bar graph represents the positive-stained areas relative to total tissue areas (data are mean ± SEM; $n = 7$). H: Analysis of hydroxyproline content in epididymal fat depots. I: Metformin lowers fasting blood glucose concentrations in HFHS-fed mice. J: Hydroxyproline concentrations in eWAT are correlated with fasting blood glucose concentrations in ob/ob mice treated with or without metformin ($R^2 = 0.5911$; $P = 0.0035$). K: Metformin inhibits the expression of fibrogenic genes including Col1a1, Col3a1, Col6a3, fibronectin, and LOX in eWAT and iWAT of HFHS-fed mice. L and M: Metformin suppresses the induction of fibrogenic regulators in eWAT and iWAT of obese mice (data are mean ± SEM; $n = 5$–6). *$P < 0.05$ vs. normal chow diet mice; #$P < 0.05$ vs. HFHS-fed mice.
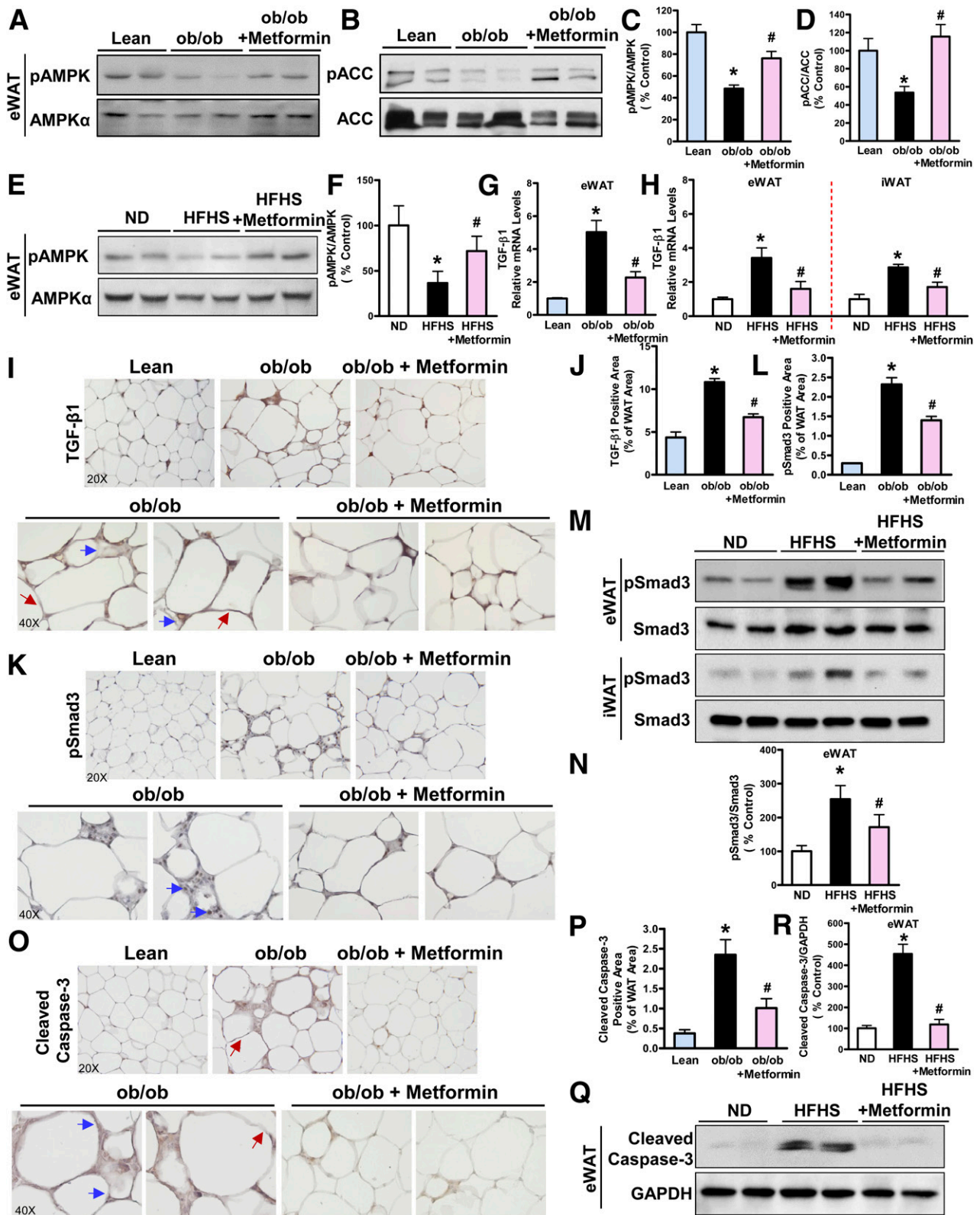
Figure 4—Metformin stimulates AMPK activity and inhibits TGF-β1/Smad3 signaling in WAT of obese mice. *A–D*: The phosphorylation of AMPK and its downstream target, ACC, is decreased in epididymal fat depots of ob/ob mice, and this impairment is restored by metformin. The data are presented as mean ± SEM (*n* = 5–7). *P < 0.05 vs. control mice; #P < 0.05 vs. obese mice. *E* and *F*: The phosphorylation of AMPK is stimulated in the eWAT of metformin-treated obese mice. *G* and *H*: The induction of TGF-β1 is suppressed in eWAT or iWAT of metformin-treated mice either on an *ob/ob* background or fed an HFHS diet. *I* and *J*: Representative immunohistochemical staining of epididymal fat sections for TGF-β1. Strong staining for TGF-β1 was visualized mainly in adipocytes (red arrows) and other cells (blue arrows) in the WAT of ob/ob mice, and this elevation was inhibited by metformin. *K–N*: Metformin reduces the increase of phosphorylated

To determine the effect of metformin on systemic glucose homeostasis, glucose tolerance tests showed that glucose clearance was significantly enhanced by metformin compared with ob/ob mice. Insulin tolerance tests also showed that systemic insulin sensitivity was increased by metformin. Integrated glucose concentrations, as calculated by the area under the curve were consistently significantly decreased. Likewise, fasting blood glucose concentrations were reduced ∼30% by metformin. A positive correlation between fat collagen content and fasting blood glucose was observed in ob/ob mice treated or untreated with metformin (r^2 = 0.6323; P < 0.01) (Fig. 1M–R).

Metformin Inhibits Aberrant Synthesis and Degradation of ECM in WAT of ob/ob Mice

To elucidate the mechanisms by which metformin attenuates pericellular fibrosis, we measured mRNA expression of collagen type I (Col1a1), type III (Col3a1), and type VI (Col6a3), all of which were shown to be highly expressed in obese adipose tissue (2). As shown in Fig. 2A, these collagens were increased five- to sevenfold in ob/ob mice, despite the basal level of Col6a3 being much higher than that of Col1a1 and Col3a1 in lean mice, as described previously (2). By contrast, overexpression of these collagens was attenuated ∼50% by metformin. Among major fibrogenic genes, expression of fibronectin, a functional integrin ligand, was also stimulated by obesity and was downregulated by metformin. LOX, a copper-dependent amine oxidase that catalyzes the covalent cross-linking of fibers through posttranslational modification of collagens, is essential for the cross-linking of collagen fibrils and fibers and the modification of biochemical and mechanical properties of the ECM (27). The antifibrotic effect of metformin was also evidenced by downregulation of fat LOX in ob/ob mice.

The development of tissue fibrosis occurs as a consequence of the dysregulation of matrix metalloproteinases (MMPs) and tissue inhibitors of MMPs (TIMPs) (28–31). To test the hypothesis that fat collagen deposition might be suppressed by metformin through altered matrix degradation, mRNA levels of MMP-2, MMP-9, MMP-13, and MT1-MMP (MMP-14), which are predominantly upregulated in obese adipose tissue (32), were assessed by quantitative RT-PCR. As shown in Fig. 2B–I, expression of different MMPs was induced 5- to 10-fold in eWAT of ob/ob mice, suggesting that the perturbation of the normal fat ECM structure and/or its replacement with newly synthesized ECM may act as a driver to promote a metabolically unfavorable fat microenvironment.

Interestingly, the induction of MMP-9 and TIMP-1 by obesity was reduced ∼60% by metformin. The protein expression and distribution of MMP-9 and TIMP-1, as assessed by immunohistochemical and immunoblotting analyses, were also reduced. No significant changes in TIMP-2 and TIMP-3 were evident among the three groups. Collectively, metformin may inhibit abnormal ECM synthesis and degradation in fat tissue, reduce LOX-related collagen cross-linking, and consequently provoke a favorable ECM flexibility.

Metformin Suppresses Aberrant ECM Remodeling in WAT of Diet-Induced Obese Mice

To better understand the potential effect of metformin on fat ECM remodeling process in obesity, we expanded our studies to a diet-induced obesity animal model. As shown in Fig. 3, hypertrophic adipocytes in epididymal and inguinal fat of mice with high fat/high sucrose (HFHS)–induced obesity were significantly reduced by metformin. Masson trichrome staining revealed that the collagen fibers surrounding adipocytes were increased seven- and threefold in the eWAT and inguinal WAT (iWAT) of HFHS-fed mice, respectively. To our surprise, the abundance of collagen deposition had a distinct feature between fat depots of obese mice: higher amounts were found in eWAT and much lower amounts in iWAT. Since the basal expression levels of Col1a1, Col6a3, and fibronectin in epididymal fat, a visceral fat associated with metabolic disease, were approximately fivefold higher than those in subcutaneous fat, it may reflect a depot-specific effect of fat fibrosis. The excessive collagen deposition of eWAT, as assessed histologically and biochemically by hydroxyproline content, was significantly reduced by metformin. The beneficial effect of metformin on interstitial fibrosis was also evidenced by reduced fibrogenic gene expression and concurrently inhibited ECM regulators such as MMP-2, MMP-9, MMP-14, and TIMP-1. The modulation of ECM components also occurred in the iWAT of metformin-treated mice. Decreased hydroxyproline concentrations in eWAT were positively correlated with lowered fasting glucose concentrations in metformin-treated HFHS-fed mice (r^2 = 0.5911; P < 0.01). Thus, metformin benefits both moderate obesity in HFHS-fed mice and severe obesity in leptin-deficient ob/ob mice.

Metformin Stimulates AMPK Activity and Inhibits TGF-β1 Signaling in WAT of Obese Mice

As shown in Fig. 4, phosphorylation of AMPK at Thr172, required for AMPK activation (33), declined ∼50% in

Smad3 in eWAT and iWAT of HFHS-fed mice. Representative immunohistochemical staining of epididymal fat sections and immunoblots for phosphorylation of Smad3 and its nuclear translocation in ob/ob mice. *O* and *P*: Metformin reduces dead adipocytes in ob/ob mice. Adipocytes of lean mice were not immunoreactive for cleaved caspase-3, an apoptotic marker, whereas more dead adipocytes (red arrows) surrounded by crown-like structure (blue arrows) in obese mice are immunoreactive for cleaved caspase-3. There was no detectable staining with a nonspecific IgG isotype control in adipose tissue sections (data not shown), indicating the specific staining for TGF-β1 expression, Smad3 phosphorylation, and cleaved caspase-3. Original magnification ×20 and ×40. *Q* and *R*: Metformin reduces cleaved casepase-3 levels in eWAT of HFHS-fed mice. The data are presented as the mean ± SEM (*n* = 7). *P < 0.05 vs. control mice; #P < 0.05 vs. obese mice.
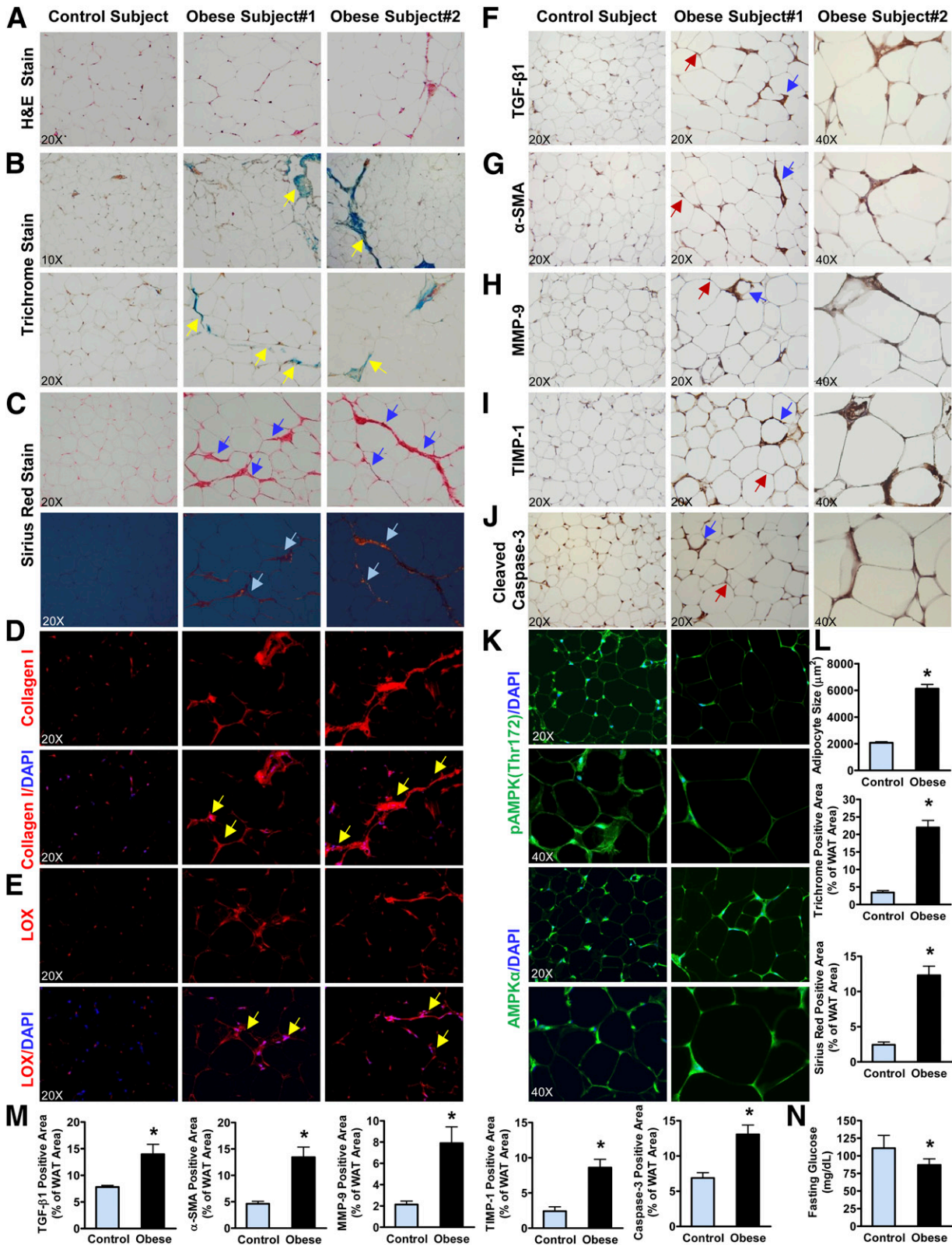
Figure 5—Pericellular fibrosis in the visceral adipose tissue of obese humans with abnormal ECM accumulation and dead adipocytes is associated with AMPK suppression and TGF-β1 induction. *A*: Representative H-E staining of omental fat depots in age-matched normal-weight subjects (*n* = 10) and obese subjects (*n* = 8). *B*: Masson trichrome staining shows minimal staining of collagen fibers in control subjects but numerous collagen fibers (yellow arrows) extended into hypertrophic adipocytes in obese subjects. *C*: Sirius Red staining shows distinct characteristics of fibril amounts and distribution between control and obese subjects. Large amounts of collagens (dark blue arrows) in the ECM surrounding hypertrophic adipocytes were observed in obese subjects. Sirius Red staining could also be visualized by polarized light microscopy, demonstrating type I and type III collagen fibers present in bundles of fibrosis (light blue arrows). *D* and

eWAT of both ob/ob mice and HFHS-fed mice, and the impairment was restored by metformin, returning to nearly normal levels. Stimulation of fat AMPK activity was further confirmed by concomitantly increased Ser79 phosphorylation of acetyl-CoA carboxylase (ACC), a well-known substrate of AMPK, consistent with metformin-induced AMPK in insulin-resistant cells (6,7,34) and in the livers of diabetic mice (8,35).

The fibrogenic regulator TGF-β binds to TGF-β receptors I and II and subsequently phosphorylates and activates downstream effectors (Smad2 and Smad3), which translocate into the nucleus and transcriptionally activate fibrogenic target genes (36–38). Because TGF-β1 is implicated in the progression of liver and heart fibrosis (36–38), we determined whether adipose tissue AMPK could be functionally linked to the modulation of TGF-β1. In agreement with elevated plasma TGF-β1 concentrations in obese humans (39), mRNA amounts of TGF-β1 were increased 5.0- and 3.4-fold in the eWAT of ob/ob mice and HFHS-fed mice, respectively. Positive staining for TGF-β1 was consistently highly elevated and located in hypertrophic adipocytes and other cells in the stromal space of ob/ob mice. Strong positive staining for Ser423/425 phosphorylation of Smad3, an indicator of TGF-β1 activity, was primarily located in nuclei of adipocytes and other cells surrounding adipocytes, which overlapped on areas of TGF-β1-positive cells. The induction of TGF-β1 expression and Smad3 phosphorylation were evident in eWAT and iWAT of HFHS-fed mice. Conversely, TGF-β1 activity, as determined by the phosphorylation and nuclear translocation of Smad3, was inhibited by metformin. Taken together, these data show that metformin activates AMPK, inactivates TGF-β1/Smad3 signaling, and ameliorates fat ECM accumulation in obesity.

MMP-mediated degradation of the ECM not only facilitates tissue remodeling but also generates bioactive cleaved peptides and releases chemokines that promote inflammation and apoptosis (31). The crown-like structure positively stained by MAC-2, a lectin that is expressed by activated macrophages (40), was dramatically increased in ob/ob mice (Supplementary Fig. 3A and B). Accordingly, an apoptotic phenotype, as determined by cleaved caspase-3, a key effector that executes the apoptotic program (41), was predominantly located in adipocytes surrounded by crown-like structures (Fig. 4O and P). Consistent with a decreased fat inflammatory response in ob/ob mice lacking Col6a3 (2), the inflammatory response and adipocyte apoptotic phenotypes in ob/ob mice were attenuated by metformin. Interestingly, mRNA levels of proinflammatory cytokines, including tumor necrosis factor-α, interleukin-1β, and MCP-1, were downregulated ~60% by metformin (Supplementary Fig. 3C). Taken together, these data show that metformin decreases TGF-β/Smad3 signaling and relieves continuous and progressive ECM remodeling in visceral adipose tissue in obesity, activities that are associated with repressed macrophage recruitment and adipocyte apoptosis.

Aberrant ECM Deposition and Pericellular Fibrosis in WAT of Obese Humans Are Associated With AMPK Inhibition and TGF-β1 Induction

To gain direct evidence for the relationship among AMPK, TGF-β1, and ECM components of fibrotic fat tissue in obese humans, histological and pathological changes in omental fat depots were characterized and compared between obese subjects ($n = 8$) and age-matched normal-weight subjects ($n = 10$). As shown in Fig. 5, H-E staining revealed that the pathologically expanded adipose tissue had much larger adipocyte areas in obese subjects than in control subjects. Masson trichrome and Sirius Red stainings showed increased numbers of collagen fibers around adipocytes of obese adipose tissue, with a higher percentage of fibrotic area, revealing fat fibrosis as a pathological process that likely reduces tissue plasticity and function in human obesity. Notably, pericellular fibrotic fat areas of obese subjects were evident in both macrophage-rich and non-macrophage–rich areas. As previously described (42), immunofluorescent analysis showed increased collagen I positive staining around adipocytes in visceral adipose tissue from obese patients, but minimal staining was seen in lean subjects. In agreement with increased fat LOX in ob/ob mice (Fig. 2A), LOX was upregulated in the omental fat of obese humans. The distribution patterns of positive

E: Representative immunofluorescent staining for collagen I (D, red) and LOX (E, red) and nuclear staining with DAPI (blue). Notably, immunostaining for collagen I displayed a pattern similar to LOX distribution in obese subjects (yellow arrows). F–I: Representative immunostaining for fibrogenic regulators and components. Omental fat tissue sections shown were serial but not always consecutive. Positive immunostaining appeared a brown color. The expression and distribution patterns of positive staining for TGF-β1 (F) and α-SMA (G) were similar to those for MMP-9 (H) and TIMP-1 (I). Notably, immunostaining for TGF-β1 was located both in adipocytes (red arrows) and in macrophage infiltration areas (blue arrows) in obese subjects. Immunostaining for α-SMA displayed the intense staining at sites of adipose tissue damage/repair, indicating the proliferation and migration of activated myofibroblast-like cells into impaired adipocytes for the secretion of excess ECM components. Immunostaining for MMP-9 and TIMP-1 also showed intense staining in the regions of macrophage-rich areas and non-macrophage–rich areas, indicating that the different cell types may be involved in collagen deposition in fibrotic adipose tissue. The minimal staining for fibrogenic regulators was present in fat depots of control subjects. J: Representative positive immunostaining for cleaved caspase-3 in dead adipocytes (red arrows) and macrophage infiltration areas (blue arrows) in the visceral WAT of obese subjects. There was no detectable staining with a nonspecific IgG isotype control in human adipose tissue sections (data not shown). K: Positive staining for phosphorylated AMPK and total AMPK (green) is localized primarily in the adipocytes of control subjects; the intensity of phosphorylated AMPK is less evident in obese subjects. Original magnification ×20 and ×40. L and M: The bar graphs represent adipocyte size and positive-stained areas relative to total tissue areas (data are mean ± SEM; $n = 7$). N: Fasting glucose concentrations in control and obese subjects (data are mean ± SEM; $n = 8–10$). *$P < 0.05$ vs. control subjects.
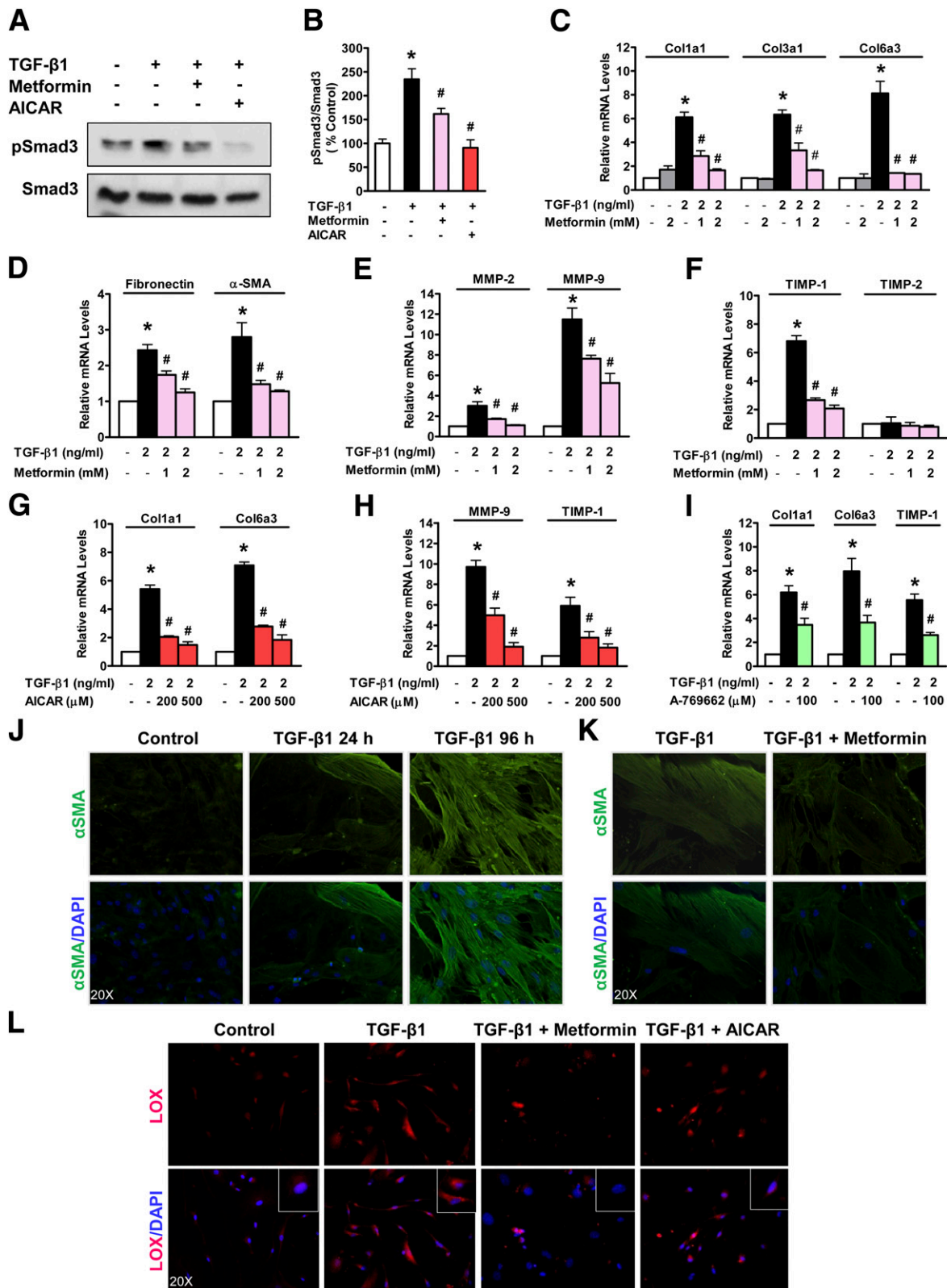
Figure 6—Pharmacological activation of AMPK suppresses the transcription of TGF-β1-dependent fibrogenic genes in vitro. *A* and *B*: A representative immunoblot (*A*) and densitometry quantification (*B*) of Smad3 phosphorylation. The cells of the SVF were isolated from epididymal fat tissue of lean C57BL/6 mice. The cells were incubated for 24 h with TGF-β1 (2 ng/mL) in the absence or presence of different AMPK activators, such as metformin (1 mmol/L) and AICAR (200 μmol/L). The phosphorylation levels of Smad3 were normalized to endogenous Smad3 levels and are expressed as a percentage of those under untreated conditions. *C–F*: Metformin suppresses the expression of fibrogenesis-related genes in response to TGF-β1. The mRNAs encoding fibrogenic components, including different types of collagen (Col1a1, Col3a1, and Col6a3), fibronectin, and α-SMA, as well as the expression of major fibrogenic regulators such as MMP-2,

staining for LOX were similar to those of collagen I positive staining, indicating that the activation of LOX-mediated collagen cross-linking may create an insoluble fibrotic matrix of collagen fibers in omental fat depots. Furthermore, immunohistochemistry of adjacent fat sections was conducted to analyze the expression and distribution of TGF-β1 and α-smooth muscle actin (SMA), a well-recognized marker of myofibroblasts. TGF-β1-positive cells were highly increased and primarily located in adipocytes and other cell types in fibrotic adipose tissue of obese subjects. Some of the inappropriately activated α-SMA-positive myofibroblast-like cells were observed. Strikingly, the distribution of TGF-β1-positive cells was overlapped by that of myofibroblast-like cells, suggesting a possible role of TGF-β1 in the differentiation of myofibroblast-like cells that were presumably derived from resident fibroblasts and other cells. Moreover, the expression and distribution of MMP-9- and TIMP-1-positive cells were increased in obese subjects, suggesting that excessive ECM degradation and remodeling may contribute to the pathological destruction of the normal matrix structure of fat depots. Similarly, the accumulated ECM deposition was associated with increased apoptotic adipocytes, as reflected by increased staining for cleaved caspase-3. Similar to inactivation of AMPK in obesity-induced insulin-resistant mice (Fig. 4), phosphorylation of AMPK was diminished in WAT of obese individuals without affecting AMPKα. Fasting glucose concentrations were elevated in obese subjects compared with controls. Collectively, suppression of AMPK and overproduction of TGF-β1 contribute to excessive fat ECM remodeling in obese patients, characterized by collagen overproduction and deposition, myofibroblast-like cell activation, and adipocyte apoptosis.

Pharmacological Activation of AMPK Inhibits TGF-β1-Induced ECM Expression in Primary Murine SVF Cells

Adipose tissue, in addition to adipocytes, contains SVF cells including preadipocytes, fibroblasts, vascular cells, and immune cells. Given the hyperactivation of adipose tissue TGF-β1 in obese mice and humans (Figs. 4 and 5), primary SVF cells isolated from epididymal fat pads of lean C57BL/6 mice were treated with TGF-β1 in an effort to develop an in vitro model that mimics in vivo conditions of obesity-induced fat fibrosis. As shown in Fig. 6A–I, mRNA amounts of Col1a1, Col3a1, and Col6a3 markedly increased six- to eightfold over the basal level upon TGF-β1 treatment. This increase was paralleled by the increase of fibronectin and

α-SMA. Like MMP-2, expression of MMP-9 was stimulated over 10-fold by TGF-β1, and the induction closely correlated with an increase of TIMP-1, but not TIMP-2. We further determined whether AMPK regulates ECM homeostasis in a cell-autonomous manner. Except the complete inhibition of Col6a3, the stimulation of fibrogenesis by TGF-β1 was reduced in a dose-dependent manner by metformin, to ∼50% the levels of TGF-β1-treated cells. In accord with the repression of collagen synthesis, metformin had an inhibitory effect on ECM degradation regulators (MMP-2, MMP-9, and TIMP-1), consistent with the in vivo effect of metformin (Fig. 2). AICAR, an analog of AMP that activates AMPK, also reduced fibrogenic response to an extent similar to that of metformin. A-769662, a specific activator of AMPK, repressed the induction of collagen and TIMP-1 by TGF-β1, although to a lesser extent. Collectively, AMPK agonists attenuate TGF-β1-induced fibrogenic response.

Metformin Inhibits TGF-β1 Activation of Myofibroblast-Like Cells In Vitro

To identify a possible source of fibrogenic cells within obese adipose tissue, the transformation of myofibroblast-like cells derived from cell origins of the SVF population was assessed upon TGF-β1 induction. As shown in Fig. 6J–L, immunocytochemical analysis showed that in the absence of TGF-β1, α-SMA-positive cells were negligible; exposure to TGF-β1 led to an increase in α-SMA-positive cells. After a 96-h incubation of TGF-β1, uniformly spindle-shaped α-SMA-positive cells were greatly increased, presuming that these cells are likely differentiated from resident fibroblasts and other cell populations in primary SVF cells. Strikingly, the amounts of α-SMA-positive myofibroblast-like cells were reduced by metformin. The reduction of α-SMA-positive cells and collagen production also coincided with the suppression of LOX. Therefore, metformin attenuates the development of myofibroblast-like cells that constitute a pool of collagen-producing cells in fibrotic adipose tissue.

A Constitutively Active Form of AMPK Is Sufficient to Reduce TGF-β1-Activated Fibrogenesis in Primary SVF Cells

To further characterize the role of AMPK in modulating ECM homeostasis, primary adipose tissue SVF cells were transduced with adenoviruses expressing control green fluorescent protein or constitutively active AMPK (CA-AMPK), a truncated mutation of AMPKα1 (α1 [1–312] T172D) that retains significant kinase activity without requiring its interaction with β- and γ-subunits (7).

MMP-9, TIMP-1, and TIMP-2, were analyzed by real-time PCR. G and H: AICAR represses the transcription of TGF-β1-dependent fibrogenic genes in a dose-dependent manner. I: A-769662 inhibits the effect of TGF-β1 on fibrogenic genes. J: TGF-β1 induces the transformation of myofibroblast-like cells in a time-dependent manner. Representative immunofluorescence images show α-SMA staining (green) and nuclear staining with DAPI (blue) in cultured SVF cells. K: Treatment with metformin (1 mmol/L) for 24 h inhibits the transformation of myofibroblast-like cells in the SVF cells exposed to TGF-β1. L: Treatment with metformin (1 mmol/L) and AICAR (200 μmol/L) for 24 h inhibits the induction of LOX in the SVF cells exposed to TGF-β1. Representative immunofluorescence images show LOX staining (red) and nuclear staining with DAPI (blue). Data are presented as mean ± SEM ($n = 3–4$). *$P < 0.05$ vs. untreated cells; #$P < 0.05$ vs. TGF-β1-treated cells.
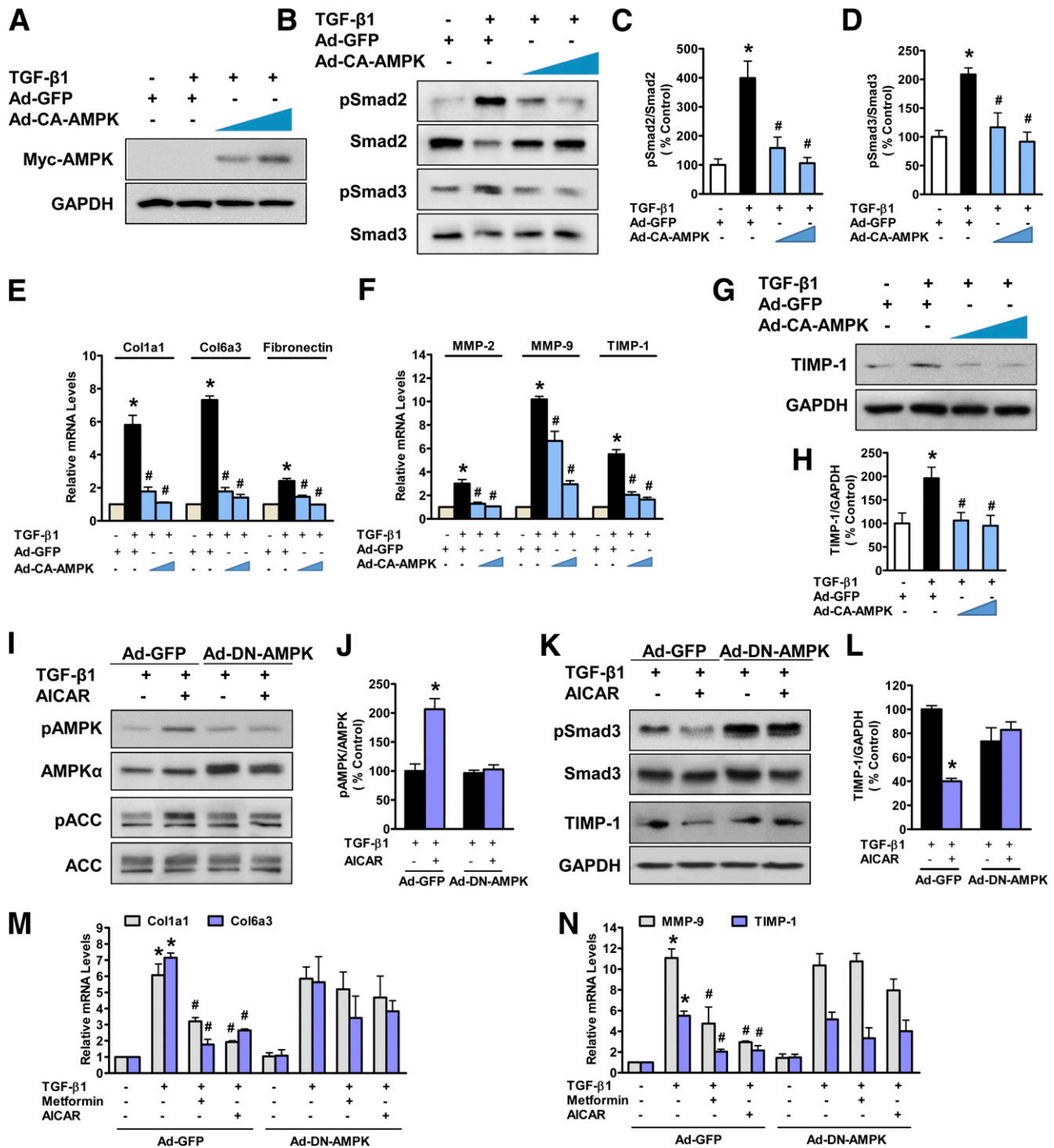
Figure 7—AMPK is necessary for metformin or AICAR to inhibit TGF-β1-dependent fibrogenesis in vitro. *A–D*: Adenovirus-mediated overexpression of CA-AMPK is sufficient to decrease the phosphorylation of Smad2 and Smad3, which are well-known downstream effectors of TGF-β1. Primary SVF cells were infected with an adenovirus expressing myc-tagged CA-AMPK (Ad-CA-AMPK) or a control adenovirus (Ad–green fluorescent protein [Ad-GFP]). Cells were treated with TGF-β1 (2 ng/mL) for another 24 h in a serum-free medium. The dose-dependent expression of CA-AMPK (~31 kDa) was detected by immunoblotting with antimyc antibody. *E–H*: TGF-β1-induced fibrogenesis is prevented by overexpression of CA-AMPK. *P < 0.05 vs. untreated cells with GFP expression; #P < 0.05 vs. TGF-β1-treated cells with GFP expression. *I* and *J*: The stimulatory effect of AICAR on AMPK is diminished by the overexpression of DN-AMPK. Primary SVF cells were infected with an adenovirus expressing DN-AMPK (Ad-DN-AMPK) or Ad-GFP. Cells were then incubated for another 24 h with TGF-β1 (2 ng/mL) in the absence or presence of metformin (1 mmol/L) or AICAR (200 μmol/L). Overexpression of DN-AMPK was confirmed by immunoblots with anti-AMPKα antibody. *K* and *L*: The effect of AICAR on TGF-β1-induced phosphorylation of Smad3 and TIMP-1 induction is abrogated by DN-AMPK. *P < 0.05 vs. TGF-β1-treated cells with GFP expression. *M* and *N*: The effect of metformin and AICAR on TGF-β1-dependent expression of fibrogenic genes is diminished by DN-AMPK. *P < 0.05 vs. untreated cells with GFP expression; #P < 0.05 vs. TGF-β1-treated cells with GFP expression.
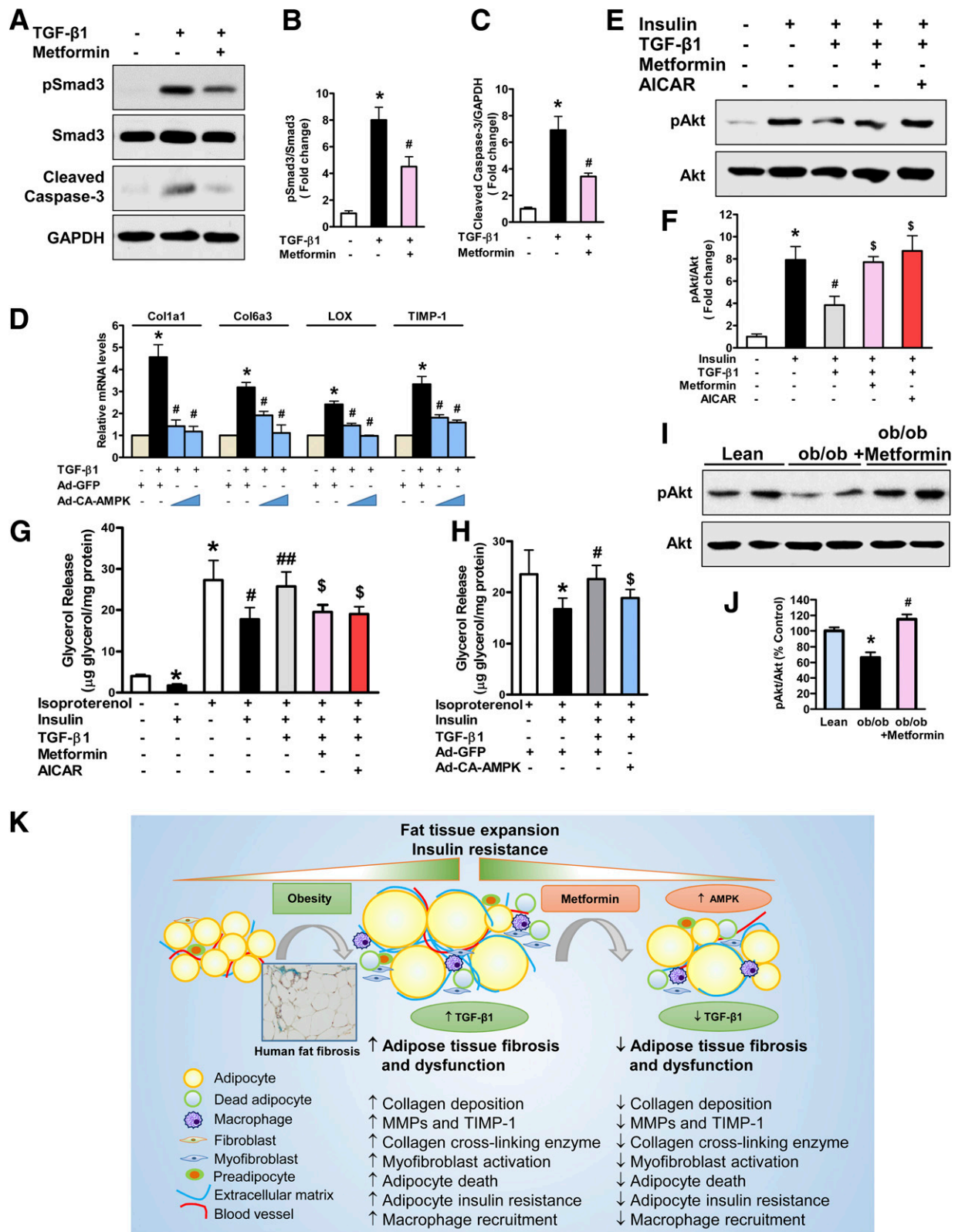
Figure 8—AMPK produces antifibrotic effects and protects against TGF-β1-induced insulin resistance in differentiated 3T3L1 adipocytes. *A–C*: Metformin represses TGF-β1-induced signaling and cell apoptosis. 3T3-L1 adipocytes on day 10 of differentiation were incubated for 24 h with 2 ng/mL TGF-β1 in the absence or presence of metformin (1 mmol/L). Representative immunoblots (*A*) and quantification of Smad3 phosphorylation (*B*) and cleaved caspase-3 (*C*) are shown. *D*: Overexpression of CA-AMPK is sufficient to suppress TGF-β1-induced expression of fibrogenic genes and the collagen cross-linking enzyme LOX. Differentiated 3T3-L1 adipocytes were infected with Ad-CA-AMPK or a control adenovirus (Ad–green fluorescent protein [Ad-GFP]) for 24 h and subsequently incubated with or without 2 ng/mL TGF-β1 for additional 24 h. The mRNA levels of Col1a1, Col6a3, TIMP-1, and LOX were determined by quantitative RT-PCR. The data are

Overexpression of CA-AMPK enhanced AMPK activity, as described previously (6,7,10). Like the metformin action (Fig. 6), overexpression of CA-AMPK effectively suppresses phosphorylation of Smad3 and subsequently mitigates the transcription of fibrogenic genes in response to TGF-β1 (Fig. 7A–H).

Metformin and AICAR Suppress TGF-β1-Induced Fibrogenic Response in an AMPK-Dependent Manner in Primary SVF Cells

The results described above suggest that activation of AMPK, either through pharmacological or genetic means, exerts an antifibrotic effect. To rigorously illustrate the requirement of AMPK for metformin actions, an adenovirus expressing dominant-negative AMPK (DN-AMPK) (6,7,10,34) was transduced into primary SVF cells. As shown in Fig. 7I–N, metformin and AICAR prevented TGF-β1-induced overproduction of collagens; their effects were largely abolished by DN-AMPK. The inhibitory effect of metformin and AICAR on MMP-9 and TIMP-1 was almost completely diminished by DN-AMPK, highlighting AMPK as a negative regulator of fibrogenesis. The data demonstrate that metformin limits excess ECM accumulation in response to TGF-β1 at least partially through AMPK.

AMPK Reduces TGF-β1/Smad3 Signaling and Improves Insulin Sensitivity in Adipocytes

Because adipose tissue TGF-β1 is implicated in the pathogenesis of obesity-induced metabolic dysfunction in humans (39), we hypothesized that adipocytes might be involved in this pathological process. To this end, differentiated 3T3L1 adipocytes were treated with TGF-β1 in the absence and presence of AMPK activators. As shown in Fig. 8, metformin largely decreased TGF-β1-stimulated phosphorylation of Smad3. Metformin-treated adipocytes were also resistant to TGF-β1-induced apoptosis,

as evidenced by reduced cleaved caspase-3. Like SVF cells (Fig. 7), CA-AMPK also blocked induction of fibrogenic genes caused by TGF-β1 in 3T3-L1 adipocytes, suggesting the effect of AMPK on fibrogenesis occurs in different cells of adipose tissue. Furthermore, TGF-β1 suppressed insulin-induced phosphorylation of Akt in adipocytes, suggesting a causal relationship between the reduction of WAT fibrosis and insulin resistance in response to metformin. Conversely, metformin or AICAR had similar effects to attenuate TGF-β1-induced insulin resistance. As an independent assessment of insulin sensitivity, insulin-mediated suppression of basal- or isoproterenol-stimulated lipolysis was measured by assessing glycerol release from 3T3-L1 adipocytes. TGF-β1 largely abolished insulin responsiveness, representing a state of insulin resistance in 3T3-L1 adipocytes. Cotreatment with AMPK activators restored the ability of insulin to inhibit lipolysis in adipocytes exposed to TGF-β1. Additionally, the ability of metformin to enhance insulin action was recapitulated by CA-AMPK. Impaired phosphorylation of Akt in eWAT of ob/ob mice was consistently substantially counteracted by metformin (Fig. 4). Thus AMPK seems to inhibit TGF-β1 activity and enhance insulin sensitivity in adipocytes.

DISCUSSION

This study provides the first biochemical evidence that metformin suppresses the TGF-β1-induced fibrogenic response at least partially through AMPK in vitro, which may explain the beneficial effects of metformin on fat fibrosis and systemic insulin resistance in obesity in vivo (Fig. 8K). In visceral WAT of obese humans, suppression of AMPK and activation of TGF-β1/Smad3 contribute to persistent and aberrant ECM remodeling, characterized by excess collagen synthesis and deposition, LOX-related collagen cross-linking, SMA-positive myofibroblast-like

---

expressed as the fold change over the basal level (mean ± SEM; n = 3–4). *P < 0.05 vs. untreated cells; #P < 0.05 vs. TGF-β1-treated cells. E and F: Pharmacological activation of AMPK rescues TGF-β1-induced insulin resistance. Differentiated 3T3-L1 adipocytes were pretreated for 24 h with 2 ng/mL TGF-β1 in the absence or presence of metformin (1 mmol/L) or AICAR (200 μmol/L). Cells were quiesced in serum-free DMEM for 5 h and subsequently stimulated with 25 nmol/L insulin for 10 min. The levels of Akt phosphorylation were normalized to those of endogenous Akt and expressed as the fold change over the basal level (mean ± SEM; n = 3). *P < 0.05 vs. untreated group; #P < 0.05 vs. insulin stimulation group; $P < 0.05, TGF-β1 treatment and insulin stimulation group. G: AMPK prevents TGF-β1-induced impairment of insulin action in adipocytes. Differentiated 3T3-L1 adipocytes were pretreated for 24 h with 2 ng/mL TGF-β1 in the absence or presence of metformin (1 mmol/L) or AICAR (200 μmol/L). Cells were serum-starved for 2 h in DMEM containing 0.2% BSA and subsequently incubated in nutrient-free Krebs-Ringer phosphate buffer containing 4% fatty-acid-free BSA for an additional 2 h in the presence or absence of 1 μmol/L isoproterenol and/or 25 nmol/L insulin, as indicated. Glycerol concentrations in medium aliquots were measured and normalized to protein concentrations in whole-cell lysates (data are mean ± SEM; n = 4). *P < 0.05 vs. untreated group; #P < 0.05 vs. isoproterenol stimulation group; ##P < 0.05 vs. isoproterenol plus insulin–treated group; $P < 0.05 vs. TGF-β1-pretreated and isoproterenol plus insulin–treated group. H: Overexpression of CA-AMPK is sufficient to restore insulin sensitivity in TGF-β1-treated adipocytes. Differentiated 3T3-L1 adipocytes were infected with Ad-CA-AMPK or Ad-GFP for 24 h. Cells were pretreated with 2 ng/mL TGF-β1 for 24 h and subjected to a glycerol release assay with 1 μmol/L isoproterenol in the absence or presence of 25 nmol/L insulin, as indicated. *P < 0.05 vs. isoproterenol stimulation group; #P < 0.05 vs. isoproterenol plus insulin–treated group; $P < 0.05 vs. TGF-β1-pretreated and isoproterenol plus insulin–treated group. I and J: Metformin enhances insulin signaling in eWAT of ob/ob mice, as reflected by the increased phosphorylation of Akt. *P < 0.05 vs. lean mice; #P < 0.05 vs. ob/ob mice. K: The proposed mechanism for the beneficial effect of AMPK and its activator metformin on adipose tissue fibrosis, a hallmark of metabolically challenged adipose tissue in obesity. Adipose tissue fibrosis is characterized by pathologically uncontrolled accumulation of ECM, induction of collagen cross-linking, activation of myofibroblasts, and adipocyte insulin resistance and death in human obesity. AMPK inhibition in adipose tissue is likely linked to TGF-β1-dependent fibrogenesis and ECM remodeling in obesity. Therapeutically, AMPK activation by metformin suppresses TGF-β1-activated fibrogenesis in adipocytes and other related cells, which in turn resolves adipose tissue fibrosis and dysfunction and improves local and systemic insulin resistance caused by obesity.

cell activation, adipocyte death, and macrophage recruitment. In mice with genetic and diet-induced obesity, metformin stimulates AMPK, reduces TGF-β1 induction and periadipocyte fibrosis, and improves local and systemic insulin resistance. Pharmacological and molecular activation of AMPK effectively inhibit TGF-β1-dependent fibrogenesis and enhance insulin sensitivity in vitro.

Concomitant Dysregulation of AMPK and TGF-β1/Smad3 Signaling Contributes to Excessive ECM Remodeling in WAT of Obese Humans and Animals

The most important implication of this study is the characterization of a previously unrecognized role of AMPK on omental adipose fibrogenesis in obese humans. Pathological changes include insoluble fibrotic matrix of collagen fibers with activation of LOX-mediated collagen cross-linking and an increase in SMA-positive cells and apoptotic adipocytes close to the fibrotic bundle. Studies by Xu et al. (13) also indicate that defective AMPK in visceral adipose tissue correlates with insulin resistance in morbidly obese patients. Increased fat mass and collagen deposition, as assessed by trichrome staining, hydroxyproline content, and fibrogenic gene expression, are likely attributable to AMPK inhibition in ob/ob mice, as AMPKα1- and AMPKα2-deficient mice exhibit adiposity and metabolic dysfunction in their adipose tissues (43). Expounding on previous observations that elevated plasma TGF-β1 correlates with adiposity in obese patients (39), this study reveals that TGF-β1 hyperactivation may contribute to the initiation of ECM remodeling in WAT of obese mice and humans. It is worth noting that ob/ob mice develop less fibrosis in response to chronic toxic liver injury than wild-type mice (44). Further research is required to understand the tissue-specific role of leptin in regulating ECM homeostasis. Since TGF-β1-positive staining was evident in both macrophage-infiltrated areas and non-macrophage–rich areas in WAT of ob/ob mice, we cannot exclude a secondary effect of fat inflammation on fat fibrosis, However, our in vitro studies delineate that TGF-β1 acts to induce adipocyte insulin resistance and stimulate myofibroblast-like cells, a major source of excessive ECM production, which is widely shared by the pathogenesis of liver fibrosis (29,30). These studies support the proposed modeling: the dysregulation of AMPK and TGF-β1 plays a causal role in promoting pathologically uncontrolled adipose tissue expansion and insulin resistance. Future studies are required to elucidate the precise role of each SVF cell type in fibrotic fat tissue.

Metformin Treatment: A Potential Applicant to Improve Adipose Fibrosis and Dysfunction in Obesity

While metformin has been the mainstay of antidiabetic therapy for over 50 years (4,5), its underlying mechanisms are not well defined. One major finding of this study is the identification of a novel function of metformin—a switch of visceral fat to subcutaneous fat properties—that is, decreased fibrogenic and inflammatory responses—which mirrors antifibrotic phenotypes in ob/ob mice lacking Col6a3

(2). Fibrogenic cell phenotypes (e.g., TGF-β1/Smad3 stimulation, LOX induction, α-SMA expression, and collagen induction in obese fat) are reduced by metformin. Since DN-AMPK abolishes the antifibrotic effect of metformin in SVF cells, metformin represses TGF-β1-induced fibrogenesis in vitro via an AMPK-dependent mechanism. Decreased fat fibrosis and lowered fasting blood glucose concentrations are highly correlated in metformin-treated mice. Metabolic improvements in metformin-treated mice may be a secondary consequence of reduced fat mass and inflammation. Fibrosis also negatively affects human adipocyte function via mechanosensitive molecules involving connective tissue growth factor and the mechanosensitive transcriptional complex YAP/TEAD (42). Further studies will investigate whether connective tissue growth factor and YAP are involved in the role of metformin in limiting fat fibrogenesis in human obesity. Therapeutically, activating AMPK by metformin may ameliorate pericellular fibrosis of WAT, systemic metabolic dysregulation, and insulin resistance. Future studies will explore whether AMPK-targeting agents such as metformin can be used to design new clinical trials to improve the health of patients with obesity or other fibrotic diseases.

In conclusion, the convergence of AMPK inhibition and TGF-β1/Smad3 activation may contribute to the development of WAT fibrosis and insulin resistance, leading to the unfavorable metabolic microenvironment in obese humans. Targeting AMPK represents a potential therapeutic approach to combat adipose tissue fibrosis and metabolic dysfunction associated with obesity.

References

1. Sun K, Kusminski CM, Scherer PE. Adipose tissue remodeling and obesity. J Clin Invest 2011;121:2094–2101
2. Khan T, Muise ES, Iyengar P, et al. Metabolic dysregulation and adipose tissue fibrosis: role of collagen VI. Mol Cell Biol 2009;29:1575–1591
3. Divoux A, Tordjman J, Lacasa D, et al. Fibrosis in human adipose tissue: composition, distribution, and link with lipid metabolism and fat mass loss. Diabetes 2010;59:2817–2825

4. He L, Wondisford FE. Metformin action: concentrations matter. Cell Metab 2015;21:159–162

5. Ferrannini E. The target of metformin in type 2 diabetes. N Engl J Med 2014;371:1547–1548

6. Zang M, Xu S, Maitland-Toolan KA, et al. Polyphenols stimulate AMP-activated protein kinase, lower lipids, and inhibit accelerated atherosclerosis in diabetic LDL receptor-deficient mice. Diabetes 2006;55:2180–2191

7. Zang M, Zuccollo A, Hou X, et al. AMP-activated protein kinase is required for the lipid-lowering effect of metformin in insulin-resistant human HepG2 cells. J Biol Chem 2004;279:47898–47905

8. Fullerton MD, Galic S, Marcinko K, et al. Single phosphorylation sites in Acc1 and Acc2 regulate lipid homeostasis and the insulin-sensitizing effects of metformin. Nat Med 2013;19:1649–1654

9. Shaw RJ, Lamia KA, Vasquez D, et al. The kinase LKB1 mediates glucose homeostasis in liver and therapeutic effects of metformin. Science 2005;310:1642–1646

10. Li Y, Xu S, Mihaylova MM, et al. AMPK phosphorylates and inhibits SREBP activity to attenuate hepatic steatosis and atherosclerosis in diet-induced insulin-resistant mice. Cell Metab 2011;13:376–388

11. Daval M, Foufelle F, Ferré P. Functions of AMP-activated protein kinase in adipose tissue. J Physiol 2006;574:55–62

12. Gauthier MS, Miyoshi H, Souza SC, et al. AMP-activated protein kinase is activated as a consequence of lipolysis in the adipocyte: potential mechanism and physiological relevance. J Biol Chem 2008;283:16514–16524

13. Xu XJ, Gauthier MS, Hess DT, et al. Insulin sensitive and resistant obesity in humans: AMPK activity, oxidative stress, and depot-specific changes in gene expression in adipose tissue. J Lipid Res 2012;53:792–801

14. Virtanen KA, Hällsten K, Parkkola R, et al. Differential effects of rosiglitazone and metformin on adipose tissue distribution and glucose uptake in type 2 diabetic subjects. Diabetes 2003;52:283–290

15. Aune UL, Ruiz L, Kajimura S. Isolation and differentiation of stromal vascular cells to beige/brite cells. J Vis Exp 2013;(73). DOI: 10.3791/50191

16. Wang QA, Scherer PE, Gupta RK. Improved methodologies for the study of adipose biology: insights gained and opportunities ahead. J Lipid Res 2014;55: 605–624

17. Madiraju AK, Erion DM, Rahimi Y, et al. Metformin suppresses gluconeogenesis by inhibiting mitochondrial glycerophosphate dehydrogenase. Nature 2014;510:542–546

18. Miller RA, Chu Q, Xie J, Foretz M, Viollet B, Birnbaum MJ. Biguanides suppress hepatic glucagon signalling by decreasing production of cyclic AMP. Nature 2013;494:256–260

19. Li Y, Xu S, Giles A, et al. Hepatic overexpression of SIRT1 in mice attenuates endoplasmic reticulum stress and insulin resistance in the liver. FASEB J 2011; 25:1664–1679

20. Sun K, Park J, Gupta OT, et al. Endotrophin triggers adipose tissue fibrosis and metabolic dysfunction. Nat Commun 2014;5:3485

21. Matsui Y, Hirasawa Y, Sugiura T, Toyoshi T, Kyuki K, Ito M. Metformin reduces body weight gain and improves glucose intolerance in high-fat diet-fed C57BL/6J mice. Biol Pharm Bull 2010;33:963–970

22. Desilets AR, Dhakal-Karki S, Dunican KC. Role of metformin for weight management in patients without type 2 diabetes. Ann Pharmacother 2008;42: 817–826

23. Tiikkainen M, Häkkinen AM, Korsheninnikova E, Nyman T, Mäkimattila S, Yki-Järvinen H. Effects of rosiglitazone and metformin on liver fat content, hepatic insulin resistance, insulin clearance, and gene expression in adipose tissue in patients with type 2 diabetes. Diabetes 2004;53:2169–2176

24. Jeong WI, Park O, Gao B. Abrogation of the antifibrotic effects of natural killer cells/interferon-gamma contributes to alcohol acceleration of liver fibrosis. Gastroenterology 2008;134:248–258

25. Yang L, Chan C-C, Kwon O-S, et al. Regulation of peroxisome proliferator-activated receptor-γ in liver fibrosis. Am J Physiol Gastrointest Liver Physiol 2006;291:G902–G911

26. Halberg N, Khan T, Trujillo ME, et al. Hypoxia-inducible factor 1alpha induces fibrosis and insulin resistance in white adipose tissue. Mol Cell Biol 2009; 29:4467–4483

27. Cox TR, Bird D, Baker AM, et al. LOX-mediated collagen crosslinking is responsible for fibrosis-enhanced metastasis. Cancer Res 2013;73:1721–1732

28. Cox TR, Erler JT. Remodeling and homeostasis of the extracellular matrix: implications for fibrotic diseases and cancer. Dis Model Mech 2011;4:165–178

29. Wynn TA. Common and unique mechanisms regulate fibrosis in various fibroproliferative diseases. J Clin Invest 2007;117:524–529

30. Schuppan D, Kim YO. Evolving therapies for liver fibrosis. J Clin Invest 2013; 123:1887–1901

31. Hu J, Van den Steen PE, Sang QX, Opdenakker G. Matrix metalloproteinase inhibitors as therapy for inflammatory and vascular diseases. Nat Rev Drug Discov 2007;6:480–498

32. Chavey C, Mari B, Monthouel MN, et al. Matrix metalloproteinases are differentially expressed in adipose tissue during obesity and modulate adipocyte differentiation. J Biol Chem 2003;278:11888–11896

33. Kahn BB, Alquier T, Carling D, Hardie DG. AMP-activated protein kinase: ancient energy gauge provides clues to modern understanding of metabolism. Cell Metab 2005;1:15–25

34. Hou X, Xu S, Maitland-Toolan KA, et al. SIRT1 regulates hepatocyte lipid metabolism through activating AMP-activated protein kinase. J Biol Chem 2008; 283:20015–20026

35. Zhou G, Myers R, Li Y, et al. Role of AMP-activated protein kinase in mechanism of metformin action. J Clin Invest 2001;108:1167–1174

36. Heldin CH, Miyazono K, ten Dijke P. TGF-beta signalling from cell membrane to nucleus through SMAD proteins. Nature 1997;390:465–471

37. Massagué J, Blain SW, Lo RS. TGFbeta signaling in growth control, cancer, and heritable disorders. Cell 2000;103:295–309

38. Wakefield LM, Roberts AB. TGF-beta signaling: positive and negative effects on tumorigenesis. Curr Opin Genet Dev 2002;12:22–29

39. Yadav H, Quijano C, Kamaraju AK, et al. Protection from obesity and diabetes by blockade of TGF-β/Smad3 signaling. Cell Metab 2011;14:67–79

40. Ho MK, Springer TA. Mac-2, a novel 32,000 Mr mouse macrophage subpopulation-specific antigen defined by monoclonal antibodies. J Immunol 1982;128:1221–1228

41. Porter AG, Jänicke RU. Emerging roles of caspase-3 in apoptosis. Cell Death Differ 1999;6:99–104

42. Pellegrinelli V, Heuvingh J, du Roure O, et al. Human adipocyte function is impacted by mechanical cues. J Pathol 2014;233:183–195

43. Zhang W, Zhang X, Wang H, et al. AMP-activated protein kinase α1 protects against diet-induced insulin resistance and obesity. Diabetes 2012;61:3114–3125

44. Leclercq IA, Farrell GC, Schriemer R, Robertson GR. Leptin is essential for the hepatic fibrogenic response to chronic liver injury. J Hepatol 2002;37:206–213